Thermal transport across nanoscale solid-fluid interfaces

Sohail Murad and Ishwar K. Puri

Citation: Applied Physics Letters **92**, 133105 (2008); doi: 10.1063/1.2905281
View online: http://dx.doi.org/10.1063/1.2905281
View Table of Contents: http://scitation.aip.org/content/aip/journal/apl/92/13?ver=pdfcov
Published by the AIP Publishing

Thermal transport across nanoscale solid-fluid interfaces

Sohail Murad[1,2] and Ishwar K. Puri[1,2,a)]
[1]*Department of Chemical Engineering, University of Illinois at Chicago, Chicago, Illinois 60607, USA*
[2]*Department of Engineering Science and Mechanics, Virginia Polytechnic Institute and State University, Blacksburg, Virginia 24061, USA*

(Received 23 January 2008; accepted 13 March 2008; published online 1 April 2008)

An explanation for the effective thermal resistance R_K can be based on the impedance to the passage of thermal phonons across an interface. We conjecture that (1) increasing the fluid pressure, and (2) making an interface more hydrophilic should facilitate better acoustic matching and thus lower R_K. Our molecular dynamics simulations confirm this. Overall, R_K decreases with increasing temperature and is inversely proportional to the heat flux. © *2008 American Institute of Physics*. [DOI: 10.1063/1.2905281]

When thermal energy is transported through a solid-fluid interface of area A, it produces a temperature discontinuity across the boundary.[1] If the heat flow Q' is small, the temperature difference across the interface ΔT is thought to be proportional to it. The effective thermal resistance $\Delta T/Q'$ is typically expressed as the Kapitza resistance,[2]

$$R_K = A\Delta T/Q' \ (\mathrm{m^2\ K/W}). \tag{1}$$

Kapitza made measurements of R_K for metal surfaces suspended in He II (the superfluid phase of ^{4}He) in the temperature range between 1.6 and 2.12 K. These and other similar experiments involving other substances and temperatures suggest that $R_K \propto T^{-\alpha}$.

The thermal resistance can be explained through the acoustic mismatch model, which assumes it to arise from the large impedance to the passage of thermal phonons across a solid-fluid interface. The acoustic impedance governing the transmission and reflection of these phonons is the product of the density and sound velocity ρc. It can be many orders of magnitude greater for a solid than for a fluid. Due to an acoustic mismatch, a large fraction of the phonons impinging upon such an interface from both sides are unable to pass through it. This model typically overpredicts the thermal resistance and is considered as an upper bound on it. The diffuse mismatch model provides a lower bound on R_K. It assumes nonspecular behavior at the interface, i.e., that all phonons are diffusively scattered. The phonon transmission probability is again related to a mismatch, in this case between the different densities of the solid-fluid states.[2]

This understanding suggests several strategies to reduce the mismatch at the interface, thus decreasing R_K and increasing Q'/A. (1) Since the product ρc increases with pressure, one approach could be to simply increase the fluid pressure to facilitate better acoustic matching, thus lowering R_K. (2) The interface could be made more solidlike by adsorbing and ordering additional fluid molecule layers,[2,3] e.g., by making the surface more hydrophilic.[4,5] For both cases, the impedance of a dense solidlike layer on the fluid side would be intermediate between the corresponding values for the solid and fluid. Once formed, its properties should be relatively pressure independent.[6] Herein, we investigate the utility of these two approaches for water-silicon systems using molecular dynamics (MD) simulations.

Our MD simulations[7,8] involve a system consisting of 1024 particles in a basic cyclically replicated parallelepiped that contains two walls. Each wall consists of 256 Si atoms (or 4×4 unit cells) that are placed at their normal equilibrium sites in a silicon crystal, as shown in Fig. 1. The axial (x-wise) dimension of the system is much larger than the transverse y and z directions to ensure that the walls explicitly influence a relatively small portion of the system adjacent to them. Water molecules are uniformly distributed between the walls and do not permeate the Si membrane during the simulations. The volume between the two walls is fixed to maintain a water density of 975 $\mathrm{kg/m^3}$ for the bulk of the simulations, although we conducted additional simulations at lower densities. The molecules are imparted with initial Gaussian velocity distributions in the solid and fluid regions, which impart different hot and cold temperatures T_h and T_c to the Si walls, and an average fluid temperature T_{av} between them.[9] These temperatures are maintained using a Gaussian thermostat, although the local water temperature varies due to the corresponding heat flux. The simulated cases are summarized in Table I.

The solution algorithm uses the quaternion method with a fifth-order Gear predictor-corrector algorithm for translational motion and a fourth-order predictor-corrector algorithm for rotational motion.[9,10] Intermolecular interactions are described by the potential model $u_{ij}=4\varepsilon_{ij}[(\sigma_{ij}/r_{ij})^{12}-(\sigma_{ij}/r_{ij})^6]+(q_iq_j)/r_{ij}$, where σ_{ij} and ε_{ij} denote the Lennard–Jones (LJ) interaction parameters, r_{ij} is the scalar distance between sites i and j, and q_i and q_j are the Coulombic charges on these sites, although not all sites have charges. The parameters σ and ε, and charges q closely represent experimental geometries, energies of ion-water complexes, and energies of solvation.[11] Lorentz–Berthelot mixing rules are used to model cross interactions[9] and the reaction field method for long-range interactions.[12,13] Water is modeled

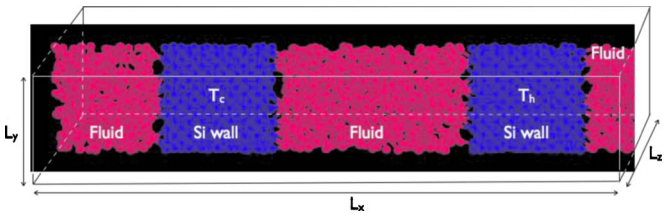

FIG. 1. (Color online) Schematic illustration of the simulation system with the dimensions $L_x\times L_y\times L_z=12.14\times2.036\times2.036\ \mathrm{nm^3}$.

a)Electronic mail: ikpuri@vt.edu.

TABLE I. Summary of the simulation cases for the $12.14\times2.036\times2.036$ nm^3, system. Here, T_h^*, T_c^*, and T_{av}^* denote the dimensionless hot Si wall, cold Si wall, and average system temperatures, respectively. Multiplying these by 800 K provides the corresponding dimensional quantities. In all cases, the walls were assumed to consist entirely of Si molecules with the analogous surfaces. Case I, however, pertains to three simulations: (a) for Si walls with the analogous surfaces, (b) for Si walls but with van der Waals interactions between water and Si reduced by an order of magnitude to make the surfaces less hydrophilic than usual, and (c) for the conditions of case I(a) in the presence of a Couette flow that is established by moving the two Si walls in opposite directions at a strain rate of 10^3 s^{-1}.

Case	T_h	T_{av}	T_c
I	1.5	1	0.5
II	1.25	1	0.75
III	1.125	1	0.875
IV	1	0.75	0.5
V	0.6	0.5	0.4
VI	0.58	0.46	0.34
VII	0.49	0.43	0.37

after the simple point-charge potential[14] and Si atoms that make up the heated and cooled walls are modeled as LJ sites.[4,15] While we have not used the more accurate Stillinger–Weber potential model[16] that considers three-body interactions to enforce the correct coordinated tetrahedral bonded structure of Si, we are nevertheless able to enforce such a structure by tethering the Si atoms to their equilibrium sites. Thus, the simpler LJ model, which is computationally less expensive, is an acceptable alternative. We segment the simulation domain into 138 transverse strips along L_x (where $\Delta x\approx0.088$ nm for each section) and average the local temperature and density of Si and H_2O molecules in each segment.

The density distributions for cases I(a) and I(b) are presented in Fig. 2. The vertical lines in the figure represent the wall boundaries. Since the Si surfaces are hydrophilic, water molecules organize over ≈1 nm at the interface into roughly three adjacent adsorbed layers. The wall hydrophilicity is varied by reducing the van der Waals interactions between water and Si molecules by an order of magnitude, as described in Table I. While this is a model system, more realistic future studies will include a layer of native SiO_2 near

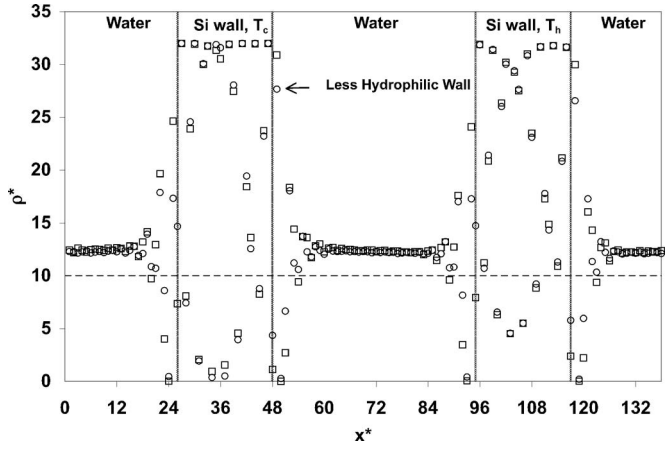

FIG. 2. The dimensionless molecular distribution ρ^* for cases I(a) and I(b) represented, respectively, by the symbols □ and ○. Multiplying ρ^* by 4.4 mol/l results and x^* by 0.088 nm provides the corresponding dimensional quantities.

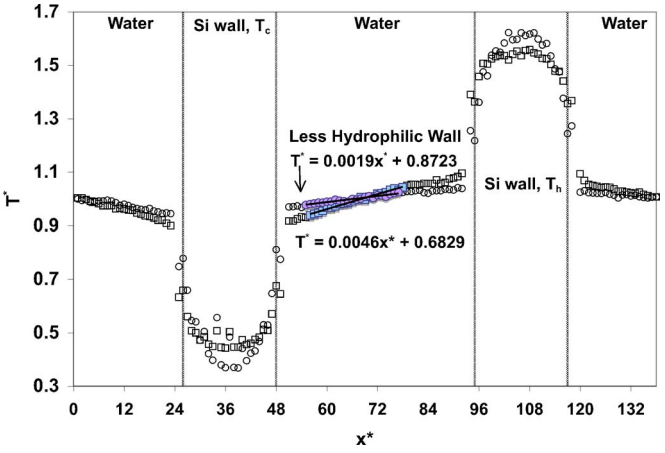

FIG. 3. (Color online) The dimensionless temperature distribution T^* for cases I(a) and I(b) represented, respectively by the symbols □ and ○. Multiplying T^* by 800 K results and x^* by 0.088 nm provides the corresponding dimensional quantities.

the surface along with its characteristic charge distribution. Making the walls less hydrophilic decreases the water density in the adsorbed layers so that the third layer of adsorbed water becomes less distinct. The bulk water density is ≈0.975 kg m^{-3} (or $\rho^*=12.3$ in the figure).

The corresponding temperature distributions are presented in Fig. 3. The overall heat flux in the system is

$$Q'/A = k_{T_{av}}\,(dT^*/dx^*)_{T_{av}}, \tag{2}$$

where both the gradient and thermal conductivity[17] $k_{T_{av}}$ are calculated at the average system temperature T_{av}. For these cases, the conductivity $k=5\times10^{-6}T^2-2.5\times10^{-3}T+0.998$ W/m K.[17] When the Si surfaces are rendered less hydrophilic, as in case I(b), the interfacial water layer is less dense and the fluid sides adjacent to the Si surfaces are less solidlike, which increase R_K. Consequently, the temperature gradient and heat flux decrease, which increases the value of ΔT across the interfacial water layer. This supports the contention that more hydrophilic surfaces that thicken the adsorbed water layer lead to enhanced thermal transport, even though the differences in the densities of the adsorbed layers immediately adjacent to the wall are relatively small.

We evaluate R_K using Eqs. (1) and (2) for which the value of ΔT is calculated across the three water layers that

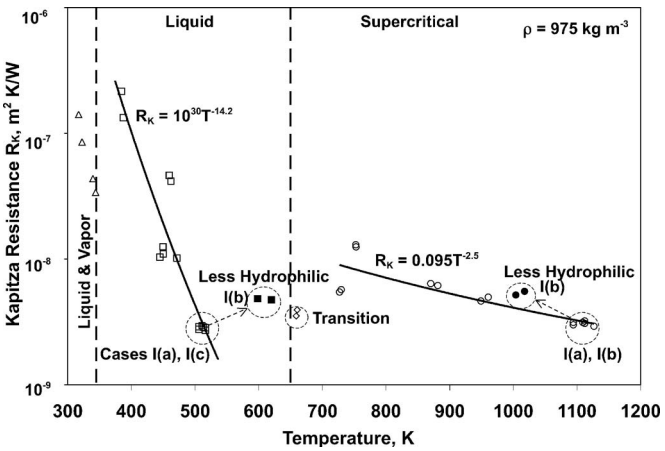

FIG. 4. Variation of the Kapitza resistance with respect to temperature for the cases listed in Table I.

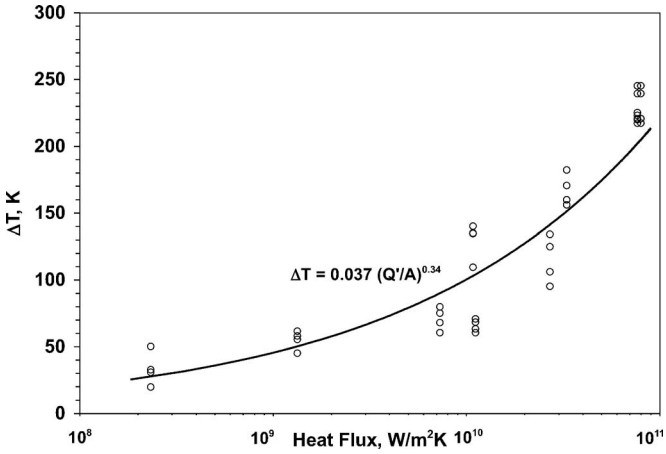

FIG. 5. Variation of the interfacial temperature difference ΔT between the fluid layers with respect to the heat flux Q'/A for the cases listed in Table I.

are typically adjacent to the Si surfaces. Its variation with respect to the temperature of the water layer immediately following any of the Si surfaces is presented in Fig. 4 for the cases listed in Table I. The temperature and pressure for these isochoric simulations follow the relation $P=2.064T-724.8$ MPa.[18,19] The simulation results include regions with coexisting liquid and vapor phases, liquid phase alone, and the supercritical fluid phase, as denoted in the figure.

Overall, the Kapitza resistance decreases with increasing temperature, which also corresponds to increasing pressure, which makes the interfacial fluid layers more solidlike, confirming our conjecture. However, as expected during phase changes, it discontinuously increases during the transition from one phase to another. The decrease in R_K with respect to increasing temperature is steeper for fluid water than for supercritical H_2O. As anticipated, the value of R_K increases for the less hydrophilic surfaces as compared to their Si counterparts. The temperature mismatch between adjacent Si and H_2O molecular layers also rises when the surface is rendered less hydrophilic. This is also explained through the decrease in the heat flux for such surfaces, since $\Delta T \propto Q'/A$.

The change in ΔT (calculated across the fluid layers adjacent to the Si surfaces) with respect to Q'/A is presented in Fig. 5 for the cases in Table I. The temperature difference is proportional to the heat flow[2] and follows the correlation $\Delta T=0.037(Q'/A)^{0.34}$. Using Eq. (1), $R_K \approx 0.037(Q'/A)^{-0.66}$, i.e., the Kapitza resistance is inversely proportional to the heat flux.

In summary, we find that the Kapitza resistance to thermal transport across a solid-fluid interface can be decreased by making the interfacial fluid layers more solidlike. This can be accomplished by increasing the fluid pressure or by adsorbing and ordering additional fluid molecule layers by making the surface more hydrophilic. While R_K decreases with increasing temperature, which for our isochoric simulations corresponds to increasing pressure, on an overall basis, it increases during the transition through phases (liquid-vapor to liquid and liquid to supercritical fluid). It is also inversely proportional to the heat flux.

S.M. was supported through the NSF Grant CBET-0730026.

[1] P. L. Kapitza, J. Phys. (USSR) **4**, 181 (1941).
[2] G. L. Pollack, Rev. Mod. Phys. **41**, 48 (1969).
[3] J. Koplik, J. R. Banavar, and J. F. Willemsen, Phys. Fluids A **1**, 781 (1989).
[4] S. Murad and I. K. Puri, Phys. Fluids **19**, 128102 (2007).
[5] L. Xue, P. Keblinski, S. R. Phillpot, S. U. S. Choi, and J. A. Eastman, J. Chem. Phys. **118**, 337 (2003).
[6] L. J. Challis, K. Dransfeld, and J. Wilks, Proc. R. Soc. London, Ser. A **260**, 31 (1961).
[7] S. Murad and J. Lin, Chem. Eng. J. **74**, 99 (1999).
[8] S. Murad and J. Lin, Ind. Eng. Chem. Res. **41**, 1076 (2002).
[9] M. P. Allen and D. J. Tildesley, *Computer Simulation of Liquids* (Clarendon, Oxford, 1987).
[10] D. J. Evans and S. Murad, Mol. Phys. **34**, 327 (1977).
[11] J. Chandrasekhar, S. F. Smith, and W. L. Jorgensen, J. Am. Chem. Soc. **106**, 3049 (1984).
[12] I. G. Tironi, R. Sperb, P. E. Smith, and W. F. Vangunsteren, J. Chem. Phys. **102**, 5451 (1995).
[13] H. J. C. Berendson, J. Postma, and W. F. van Gunsteren, in *Intermolecular Forces*, edited by B. Pullman (Reidel, Dordrecht, 1981).
[14] R. O. Watts, Mol. Phys. **28**, 1069 (1974).
[15] S. Murad and I. K. Puri, Nano Lett. **7**, 707 (2007).
[16] F. H. Stillinger and T. A. Weber, Phys. Rev. B **31**, 5262 (1985).
[17] IAPWS, *Revised Release on the IAPS Formulation 1985 for the Thermal Conductivity of Ordinary Water Substance*, Vol. 23 (International Association for the Properties of Water and Steam, London, 1998).
[18] A. Saul and W. Wagner, J. Phys. Chem. Ref. Data **18**, 1537 (1989).
[19] W. Wagner and A. Pruss, J. Phys. Chem. Ref. Data **31**, 387 (2002).